

AD-A103 572 RUTGERS - THE STATE UNIV. PISCATAWAY NJ DEPT OF ELECT--ETC F/G 9/5  
INVESTIGATION OF THE TRANSPORT, DIELECTRIC AND SWITCHING PROPERTY--ETC(U)  
JUL 81 B LALEVIC DAAG29-80-C-0072

UNCLASSIFIED

ARO-13978-2-P

NL

100-  
AD-A103 572

END  
DATE FILMED  
0-81  
DTIC

AD A103572

(1) ARO/13978.2-P

REPORT DOCUMENTATION PAGE			READ INSTRUCTIONS BEFORE COMPLETING FORM	
1. REPORT NUMBER <i>b</i>	2. GOVT ACCESSION NO. <i>AD-A103572 (1)</i>	3. RECIPIENT'S DATA JG NUMBER		
4. TITLE (and Subtitle) Investigation of the Transport, Dielectric and Switching Properties of Metal-Oxide (MOX) NbO <sub>2</sub> Suppressor Devices.			5. TYPE OF REPORT & PERIOD COVERED Final Report 1 Dec 1977-19 Apr 1981	
7. AUTHOR(S) <i>SP/ B. Lalevic</i>	8. PERFORMING ORG. REPORT NUMBER <i>(12) 15</i>		9. CONTRACT OR GRANT NUMBER(S) DAAG29-79-C-0025 DAAG29-80-C-0072, <b>DAAG 29-78-G-0035</b>	
11. CONTROLLING OFFICE NAME AND ADDRESS U. S. Army Research Office Post Office Box 12211 Research Triangle Park, NC 27709	12. REPORT DATE <i>(1) 15 July 1981</i>		13. NUMBER OF PAGES	
14. MONITORING AGENCY NAME & ADDRESS (if different from Controlling Office) <i>(12) 25 LEVEL</i>	15. SECURITY CLASS. (of this report) Unclassified		16a. DECLASSIFICATION/DOWNGRADING SCHEDULE	
16. DISTRIBUTION STATEMENT (of this Report) Approved for public release; distribution unlimited.	17. DISTRIBUTION STATEMENT (of the abstract entered in Block 20, if different from Report) <i>IA</i>		DTIC ELECTED S SEP 2 1981 H	
18. SUPPLEMENTARY NOTES The view, opinions, and/or findings contained in this report are those of the author(s) and should not be construed as an official Department of the Army position, policy, or decision, unless so designated by other documentation.				
19. KEY WORDS (Continue on reverse side if necessary and identify by block number) High pulse power switching, switching parameters, switching mechanism, transport properties, dielectric properties				
20. ABSTRACT (Continue on reverse side if necessary and identify by block number) On separate pages.				

N  
410-516

INVESTIGATION OF THE TRANSPORT, DIELECTRIC AND SWITCHING  
PROPERTIES OF METAL-OXIDE (MOX)  $\text{NbO}_2$  SUPPRESSOR DEVICES

Final Report

U.S. Army Research Office

Grants DAAG29-78-G-0025 and DAAG29-80-C-0072

Dr. B. Lalevic  
Professor of Electrical Engineering  
Department of Electrical Engineering  
College of Engineering  
Rutgers University  
P.O. Box 909, Piscataway, NJ 08854

Approved for Public Release

Distribution Unlimited

The view, opinions and/or findings contained in this report are those of  
the author and should not be construed as an official Department of the  
Army position, policy, or decision, unless so designated by other documentation.

81 9 01 107

## ABSTRACT

$\text{NbO}_2$  threshold switching devices have shown excellent capability as suppressor of high voltage, high current pulses when other more conventional devices cannot be applied. Stable and reproducible switching performance was observed in the Bi- $\text{NbO}_2$ -Bi device structure. Improvements in the device performance is attributed to the Bi diffusion into  $\text{NbO}_2$ . This was shown by the Auger electron spectroscopy (AES) measurements.

The pulsed switched single crystal devices can withstand pulse duration between 0.1-3.0  $\mu\text{sec}$ , repetition rate of  $10^3$  Hz and current intensities of 26 Amps. peak with applied pulse duration of 20  $\mu\text{sec}$ . single shot. Maximum energy was of the order of 2.52 joules. Polycrystalline devices passed maximum currents of 45 Amps. A final recommended device configuration is Au-Cr-Bi- $\text{NbO}_2$ -Au with 500° A films of each Au, Cr and Bi. It was found that Cr acted as a barrier and prevented Au diffusion. This was confirmed by AES measurements. A better adhesion and prolonged device life time was achieved. In the final device configuration a layer of  $\text{SiO}_2$  was evaporated over the device to eliminate sparking and contamination effects.

Results and interpretation of the switching phenomena and other properties are presented. The following characteristic switching parameters are determined as a function of several variables, threshold voltage  $V_{th}$ , holding voltage  $V_h$ , holding current  $I_h$ , delay time  $\tau_d$ , recovery time  $\tau_{rec}$  and current rise time  $t_I$ . Further experiments were performed to determine the nature of switching mechanism. These experiments included (1) Transient on Characteristics (TONC); (2) RF oscillation; (3) Thermal radiation; (4) Thermoelectric power; and (5) Trap concentration and energy position. Results of the above experiments

indicate the electronic nature of the switching mechanism.

Transport and dielectric properties of polycrystalline and single crystal  $\text{NbO}_2$  were studied in the MIM configuration as a function of the applied field, frequency and temperature. Two well-defined conduction states and a final state in the dielectric breakdown were established. Devices with evaporated Bi electrodes showed the existence of a Schottky barrier of height 1.2 eV and the thermal activation energy 0.48 eV for the non-formed conduction state. the I-V-T, C-V, C-V-f and C-T-f results were explained by the MIM model with the Schottky barrier at the metal-insulator interfaces, complemented by the modified Debye model at higher frequencies.

Accession For	LTIS GR&R
DTIC Typ	U
Unauthorised	<input checked="" type="checkbox"/>
Justification	<input type="checkbox"/>
By	
Distribution	
Availability Codes	
Dist	4.00 and/or Iperial

A

Participants

Dr. B. Lalevic, Professor of Electrical Engineering

Dr. M. Gvishi, Visiting Scientist from the Israeli Ministry of Defense

Mr. M. Shoga, Graduate Student

Mr. M. Yousuf, Graduate Student

Ph.D. Dissertations

Munir Shoga, "Electronic Properties of the High Current, High Voltage NbO<sub>2</sub> Suppressor Devices," Rutgers University, May 1981.

Moustafa Yousuf, "Methods of Specification of Trapping Centers with Applications to NbO Switching Devices," Rutgers University, October 1981.

Publications

1. B. Lalevic, M. Gvishi and M. Shoga, "Schottky Barrier Effects on the Electrical Properties of the Bi-NbO<sub>2</sub>-Bi System," *Physica Status Solidi*, 56a, 79 (1979).
2. B. Lalevic, M. Gvishi, M. Shoga and S. Levi, "Stabilization of Metal-Oxide Bulk Switching Devices with Diffused Bi Contacts," *IEEE Proceedings, 2nd International Pulse Power Conf.*, Lubbock, Texas, June 1979.
3. B. Lalevic and M. Shoga, "Relaxation Oscillation in NbO<sub>2</sub> Thin Film Switching Devices," *Thin Solid Films*, 75, 199 (1980).
4. G. Vezzoli, L. Doremus, S. Levy, G. Gaule, B. Lalevic and M. Shoga, "The On State of Single Crystal and Polycrystalline NbO<sub>2</sub>," *J. Appl. Phys.*, 52(2), 833 (1981).
5. M. Yousuf and B. Lalevic, "Investigation of Trapping Centers in Single Crystal NbO<sub>2</sub> by Admittance Spectroscopy," *J. Appl. Phys.*, accepted for publication.

$\text{NbO}_2$  threshold switching devices have shown excellent capability as suppressor of high voltage, high current pulses when other more conventional devices cannot be applied. Results and interpretation of the switching phenomena and other properties are briefly reviewed.

#### Device Performance

The following characteristic switching parameters are determined as a function of several variables, threshold voltage  $V_{th}$ , holding voltage  $V_h$ , holding current  $I_h$ , delay time  $\tau_d$ , recovery time  $\tau_{rec}$  and current rise time  $t_I$ . Further experiments were performed to determine the nature of switching mechanism.

$V_{th}$  was found to be dependent on the rate of applied voltage pulse and pulse width, i.e. on the power input. However, using shorter pulses 0.1  $\mu\text{sec}$ . and electrode configuration Au-Cr-Bi- $\text{NbO}_2$ , the threshold voltage  $V_{th}$  was found to be reproducible.

Stable and reproducible switching performance was observed in the Bi- $\text{NbO}_2$ -Bi device structure. Improvements in the device performance is attributed to the Bi diffusion into  $\text{NbO}_2$ . This diffusion was confirmed by the Auger electron spectroscopy (AES) measurements, as shown in Fig. 1.

The pulsed switched single crystal devices can withstand pulse duration between 0.1-3.0  $\mu\text{sec}$ ., repetition rate of  $10^3$  Hz and current intensities of 26 Amps. peak with applied pulse duration of 20  $\mu\text{sec}$ . single shot. Maximum energy was of the order of 2.52 joules. Polycrystalline devices passed maximum currents of 45 Amps. Further improvement was achieved by deposition of 500° A of Cr over Bi electrode. Cr layer prevents diffusion of the outer Au electrode in Bi and  $\text{NbO}_2$ , as shown in Fig. 2. Diffusion of Au in  $\text{NbO}_2$  causes a deterioration of a device as shown by comparative studies of Auger analysis and device performance.

Au-Cr-Bi-NbO<sub>2</sub> devices have been cycled  $4 \times 10^4$  times from the threshold voltage 500 V to 2000 V using 1 to 3.0  $\mu$ sec. pulses with max. current of 20 Amps. before the device failed.

One of the requirements for the protective device is to be able to sustain 20 Amps. with 5  $\mu$ sec. pulses which is very close to the above result.

Similar devices were switched 500 times before failing, using 20 nsec. pulses with the amplitude of 2000 V and peak current of 45 Amps. One of the requirements for the protective device is to sustain 400 Amps. at 400 nsec. However, a lack of proper pulse generator for the above current has prevented us to test our devices at that power level.

Current rise time is less than .8 n sec. or  $\frac{dI}{dt} = 310 \text{ A}/\mu\text{sec}$ . which represents a lower limit of our equipment and yet it is in agreement with proposed requirements.

A final recommended device configuration is Au-Cr-Bi-NbO<sub>2</sub>-Au with 500° A thick films of each Au, Cr and Bi. It was found that Cr acted as a barrier and prevented Au diffusion which led invariably to the deterioration of device performance. This was confirmed by Auger Electron Spectroscopy measurements. A better gold wire adhesion and prolonged device lifetime was achieved in the above configuration. In the final device configuration a layer of SiO<sub>2</sub> was evaporated over the device to eliminate sparking and contamination effects. Device was packed in a MODPACK module with a microswitch with eight positions as shown in Fig. 3.

#### Switching Mechanism

The following measurements were performed in order to establish the nature of switching mechanism in NbO<sub>2</sub> devices:

- (1) Transient On-Characteristics-TONC
- (2) R-F Oscillations

- (3) Diagnostic pulse technique in the "off" state
- (4) Measurements of traps
- (5) Balberg type double pulse measurements

These experiments were brought to a successful conclusion except for the Balberg double pulse measurements where the fluctuation of the high voltage pulses were interfering with measurements.

#### Recovery Phenomena and TONC Results

Diagnostic pulses provided very fast interruption into the on-state revealed plateau regions in device interruption voltage level versus time. The resulting I-V curve showed a transitional region between the essentially linear metal-like on-state, and a lower conductance subregime of the on-state. The trapped carrier life time or emission time measured from continuous wave (CW) studies for polycrystalline is 250-350 nsec., were at least  $5 \times 10^9$  carriers undergo recombination and emission time of 10-20 nsec. for a single crystal device. A tentative conclusion was drawn on the current decay mechanism during the transition from the on to the off resistance state.

The minimum recovery time of 1.0  $\mu$ s obtained and interpreted as the life time as free carrier  $\tau_2$ . A recovery curve (plot of the ratio of the reswitching threshold to the initial threshold versus zero voltage interruption time) is shown in Fig. 4. These results and the results of the double pulse experiment indicate a recovery which is symmetric for both polarities; the recovered on-current is constant as the reswitching voltage is increasing and the recovery process is not entirely complete even after values of  $\tau_{V=0}$  of several hundred  $\mu$ sec. This ultra long final recovery tail is likely to be the thermal equilibrium time constant.

The character of the I-V dependence during the decreasing voltage excursion will be discussed according to Fig. 5 where we distinguished five different regions of behavior.

Region I: (0-10 ns) This region probably is related to the free carrier response time which is limited by the dielectric relaxation time  $\tau = RC = (35V/0.2A \times 5 \times 10^{-12}) = 10^{-9}$  sec. Thus a few ns occur before the voltage drop is actually observed.

Region II: (10-50 ns, R=125 ohm) This interval displays linear characteristics and thus appears to represent the true I-V characteristics of the metal-like on-state of NbO<sub>2</sub>. The region from 20 to 30 ns corresponds to the first plateau region in the V versus t data and if we may tentatively speculate, may represent the beginning of a conduction band emptying into an unoccupied shallow donor state possibly via a tunneling mechanism. Region II could be approximately extrapolated through the origin.

Region III: (50-60 ns, R=330 ohm) This region is associated with behavior at voltages under the holding value and may be associated with behavior created by band bending between the two plateau regions.

Region IV: (70-90 ns, R=20 ohm) This clearly is the transitional region from the high current metal-like regime to the lower conductance subregime. It corresponds to the second plateau region in Fig. 6c. This plateau region is far more pronounced at higher overvoltage than at the zero overvoltage event shown in Fig. 6b. There is no change in the plateau structure as the applied voltage is increased from 1330 V to 2200 V, therefore a range of almost 900 V in overvoltage has no apparent effect on the knee structure of the transitional regime (Region IV). Thus, we assume that traps are saturated at the threshold, and that the knee structure is indicative of trap emptying.

At high overvoltage the bands are more populated with free carriers, and are apparently more perturbed, overlapping, and/or interacting. Thus, overvoltage can promote enhanced tunneling behavior while it would also be observed during decay or relaxation (as in Fig. 6) and reflected as plateau regions. We interpret the transitional regime to be caused by a voltage that is less

than the holding value for an excess of the trap emission time.

At low frequency (120 Hz) single crystal devices of  $\text{NbO}_2$  do not show the same type of down-voltage on-state I-V behavior as do the polycrystalline materials. Instead of displaying the presence of a pronounced negative region and of a switch-off transient, the single crystal curve tracer data reflects the current-voltage characteristics. The voltage at the knee condition in the I-V characteristics corresponds consistently rather closely to the voltage for the inflection point between Regions II and III (at 50 ns into the interruption in Fig. 5. This may add credence to the suggestion that the increased differential resistance of Region III contrasting Region II may be due to falling beneath the holding voltage and consequent decay of some carriers.

Region V: (100-120 ns,  $R=750 \text{ ohm}$ ) The I-V regime corresponding to Region V is referred herein as the lower conductance subregime of the on-state. In the present interpretation this region could correspond to hopping conduction in a trapping level or band. Such a band can only accept free carriers from the conduction band after the trapped carrier emission time ( $\tau_1 = 10-20 \text{ ns}$ ) has been exceeded. This means that the carriers which were trapped during the pre-switching regime have had enough time to decay in order to leave trapping sites vacant for the capture and recombination of carriers which were in the conduction band during the ohmic Regions II and III of Fig. 5. The manner in which a trapping state can arise from a crystal chemical standpoint in non-stoichiometric  $\text{NbO}_2$  is described later. Alternatively, Region V may be associated with residual trapped charge and consequent high resistance regions near the contacts provided there exists an asymmetry in charge distribution.

The change in current during the transitional regime from 60 to 100 ns into the interruption is about 84ma, or  $\Delta I/\Delta t = 83 \times 10^{-3} \text{ A}/40 \times 10^{-9} \text{ s} = 2 \times 10^6 \text{ A/s}$  or  $2 \cdot 10^6 (\text{coul/sec})/\text{sec}$ . Thus, the rate of electron deceleration is  $1 \times 10^{25} \text{ electrons/sec}^2$ .

The rate of voltage change during this interval is  $-4V/40 \times 10^{-9} s = 1 \times 10^{18} V/s$ . Dividing tells us that for every volt decrement in on-potential there will occur  $1 \times 10^{17}$  electron/sec decay or in an interval of 40ns in which the voltage is decreased by 4V (the transitional regime in Fig. 5), these will occur  $4 \times 1 \times 10^{17} \times 40 \times 10^{-9} = \text{about } 1.6 \times 10^{10}$  electron recombinations. We now assume that these recombinations are accomplished to trapping sites furnished by the niobium ions which compensate for the oxide non-stoichiometry. From a crystal chemistry standpoint we can write the non-stoichiometric form of  $\text{NbO}_2$  as  $\text{NbO}_{2-x}$  and retain charge balance by assuming some fraction of cations to be in a lower oxidation state than +4.

Thus we write  $\text{NbO}_2$  as  $[\text{Nb}^{4+}]_y [\text{Nb}^{4+}_{(1-y)}] [\text{O}^{2-}_{(2-x)}]$

We know from previous work that the non-stoichiometric compound  $\text{NbO}_{1.87}$  represents the lowest oxygen content for reproducible threshold switching of polycrystalline device. Therefore, if we take  $x=0.13$  and solve the charge balance equation, we arrive at  $y=0.87$ . This suggests that at  $y=0.87$  there will exist too many  $\text{NbO}_2$  trapping centers in order that trap-saturation or near saturation could be accomplished by the electric field. Assuming no other trapping mechanism this implies that the ratio of  $\text{Nb}^{+4}$  to  $\text{Nb}^{+2}$  must be greater than  $0.87/0.13=6.1$ .

#### Trapping Centers

Investigation of trap parameters in single crystal Niobium Dioxide is performed employing admittance spectroscopy method. From conductance and capacitance measurements versus temperature at different fixed frequencies, five trap levels with energies between 0.25-0.435 eV were identified. Other characteristic parameters such as trap density, their capture cross section and emission rate were also determined. Measured values of these parameters indicate the existence of two groups of traps, as shown in Table I.

TABLE I

Numerical values of trap parameters in single crystal  $\text{NbO}_2$ , as determined by Admittance Spectroscopy technique.  $E_t$  represents the trap energy level with reference to the bottom of conduction band,  $N_t$  is the trap density,  $\sigma_n$  is the capture cross-section and  $e_{no}$  is the emission rate of the trap. Traps are denoted by letters A to E as shown in Figs. 1-4.

<u>Trap</u>	<u><math>E_t</math> (eV)</u>	<u><math>N_t</math> (<math>\text{cm}^{-3}</math>)</u>	<u><math>\sigma_n</math> (<math>\text{cm}^2</math>)</u>	<u><math>e_{no}</math> (<math>\text{sec}^{-1}</math>)</u>
A	0.435	$8 \times 10^{17}$	$3.8 \times 10^{-14}$	$9.2 \times 10^{11}$
B	0.393	$\sim 3.88 \times 10^{19}$	$2.7 \times 10^{-18}$	$6.5 \times 10^7$
C	0.36	$4.6 \times 10^{19}$	$3.75 \times 10^{-19}$	$8.4 \times 10^6$
D	$0.25 + 0.013$	$\sim 1.27 \times 10^{19}$	$4.19 \times 10^{-21}$	$1 \times 10^5$
E	$0.3 + 0.01$	$\sim 1.099 \times 10^{19}$	$1.635 \times 10^{-20}$	$3.41 \times 10^5$

#### RF Oscillations

Further indications that switching process in  $\text{NbO}_2$  devices is electronic in nature comes from the observed RF oscillations. The observed oscillations at a given bias and temperature are very stable. A model of CCNR device oscillations is developed and limit cycle for different bias voltages were derived.

#### Conduction in the "On" State

Three types of measurements were performed in order to determine if the conduction in the on state occurs through a formation of a hot filament or if it is uniform under the electrode area. These measurements are:

- (1) Thermal radiation measurements
- (2) Thermoelectric power measurements
- (3) Current dependence on electrode area in the on state.

Measurements at 1 and 3 indicate a filament formation while the thermoelectric power could only be explained if the volume under electrodes is conducting.

### Thermal Radiation Measurements

Thermal emittance measurements were performed on a single crystal device with evaporated electrodes in the configuration Au-Cr-Bi-NbO<sub>2</sub>. Barns Engineering Infrared Radiometric Microscope with an objective lense X74 (resolution of 15  $\mu\text{m}$ ) and temperature sensitivity of 0.5° C, was used for this purpose.

Temperature measurements were recorded while scanning in a direction perpendicular (to the assumed existing channel of conduction) across two surface contacts between which switching is taking place. Results were plotted using the computer and are shown in Fig. 7. Temperature distributions exhibit a pronounced maximum and gradual fall off away from the center. They also have a plateau type region in the highest temperature regions and 130 mAmps. Plateau regions of constant temperature are more pronounced at the higher currents 100, 120 and 130 mA; the width of these regions ranges between 50-100  $\mu\text{m}$ . For 130 mA temperature profile, a maximum temperature of 160° C occurs in a case where  $r \leq 50 \mu\text{m}$ .

Thermoelectric measurements have given the following results:

(1) Before switching:

$$R = 10 \text{ k} \Omega \quad \alpha_1 = 250 \mu\text{V/deg.}$$

$$\sigma \sim 5.9 \times 10^{-6} (\Omega \text{cr}^{-1})$$

(2) After switching:

$$R = 2 \text{ k} \Omega \quad \alpha_2 = 180 \mu\text{V/deg.}$$

If one assumes the conduction under the electrode area one can calculate  $\alpha_1 - \alpha_2$  which gives the value of

$$\alpha_1 - \alpha_2 = 110 \mu\text{V/deg.}$$

which is close to the experimental value of 70  $\mu\text{V/deg.}$  However, assuming a filamentary conduction with a filament radius of 100  $\mu\text{m}$  one obtains

$$\alpha_1 - \alpha_2 = 0.616 \text{ mV/deg.}$$

which is much larger than the observed value and represents a problem which could be solved by many other methods.

#### Transport and Dielectric Properties

Transport and dielectric properties of polycrystalline and single crystal  $\text{NbO}_2$  were studied in the MIM configuration as a function of the applied field, frequency and temperature. Two well defined conduction states and a final state in the dielectric breakdown were established. Devices with evaporated Bi electrodes showed the existence of a Schottky barrier of height 1.2 eV and the thermal activation energy 0.48 eV for the non-formed conduction state. The I-V-T, C-V, C-V-f and C-T-f results were explained by the MIM model with the Schottky barrier at the metal-insulator interfaces, complemented by the modified Debye model at higher frequencies.

In formed conduction state Schottky barrier has been eliminated upon switching and conduction is space-charge limited. An increase in conductivity was observed, and a decrease in thermal activation energy to .097 eV.

In the final stage of dielectric breakdown, polycrystalline devices showed a low 0.059 eV thermal activation energy. Results of  $G(\omega)$  versus f measurements indicated a large dc component in the range 0 to 5 MHz. I-V characteristics in the final stage were nearly ohmic. Reduction in thermal activation energy and a linear increase in current with the applied voltage indicate that the breakdown occurs through the formation of a metallic or highly degenerate semiconducting filamentary path. This is corroborated by the finding that the resistance in the final stage is independent of electrode area.

#### Suggestions for the Improvement of Device Performance

- 1) Controlled diffusion of Bi into  $\text{NbO}_2$ . Depth and lateral diffusion of Bi should be enhanced at higher temperatures. Lateral diffusion should prevent sparking while depth diffusion will control the threshold voltage.

2) Implantation of a buried lower resistance layer and its subsequent annealing and diffusion. This is expected to improve the current carrying capacity by widening current filament and to control the threshold voltage by the depth of non-doped portion of  $\text{NbO}_2$  wafer. It should also suppress sparking which is in general due to the percolation near the surface. Materials considered for doping are Bi, Sb, V and Ta. Experiments will be performed in conjunction with the Auger spectroscopy.

3) Heat sinking. Improvement in heat exchange will prolong the device life time. It has been shown in our previous experiments that the heat dissipation caused by on-state current was responsible for device failure. When current was limited by an SCR the device life time was prolonged by several orders of magnitude. Different substrates, like sapphire, should be tested.

4) Encapsulation has proved to be beneficial. It improves probably overall heat exchange, prevents sparking and deterioration of a device due to the environment.

NbO<sub>2</sub> on NbO  
POLYCRYSTALLINE  
BATCH #106

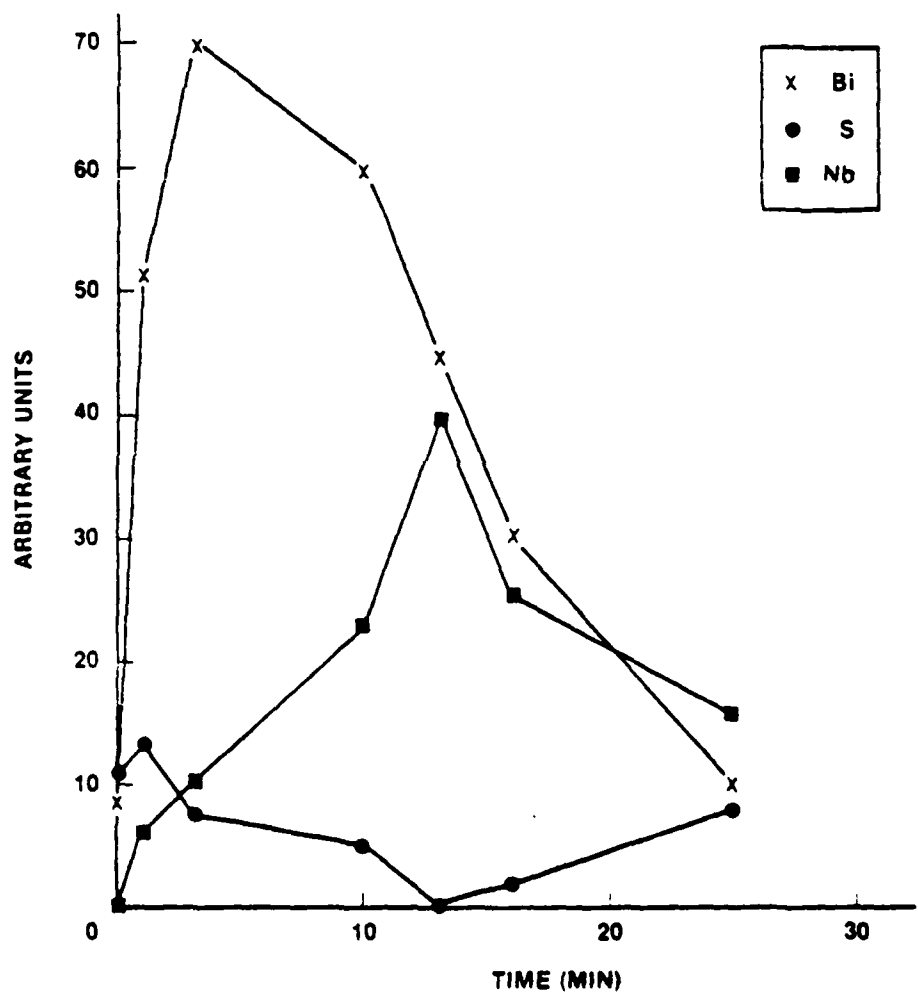


Figure 1. ABS measurements for a device in the structure Bi-NbO<sub>2</sub>-Bi.

a) Before Switching

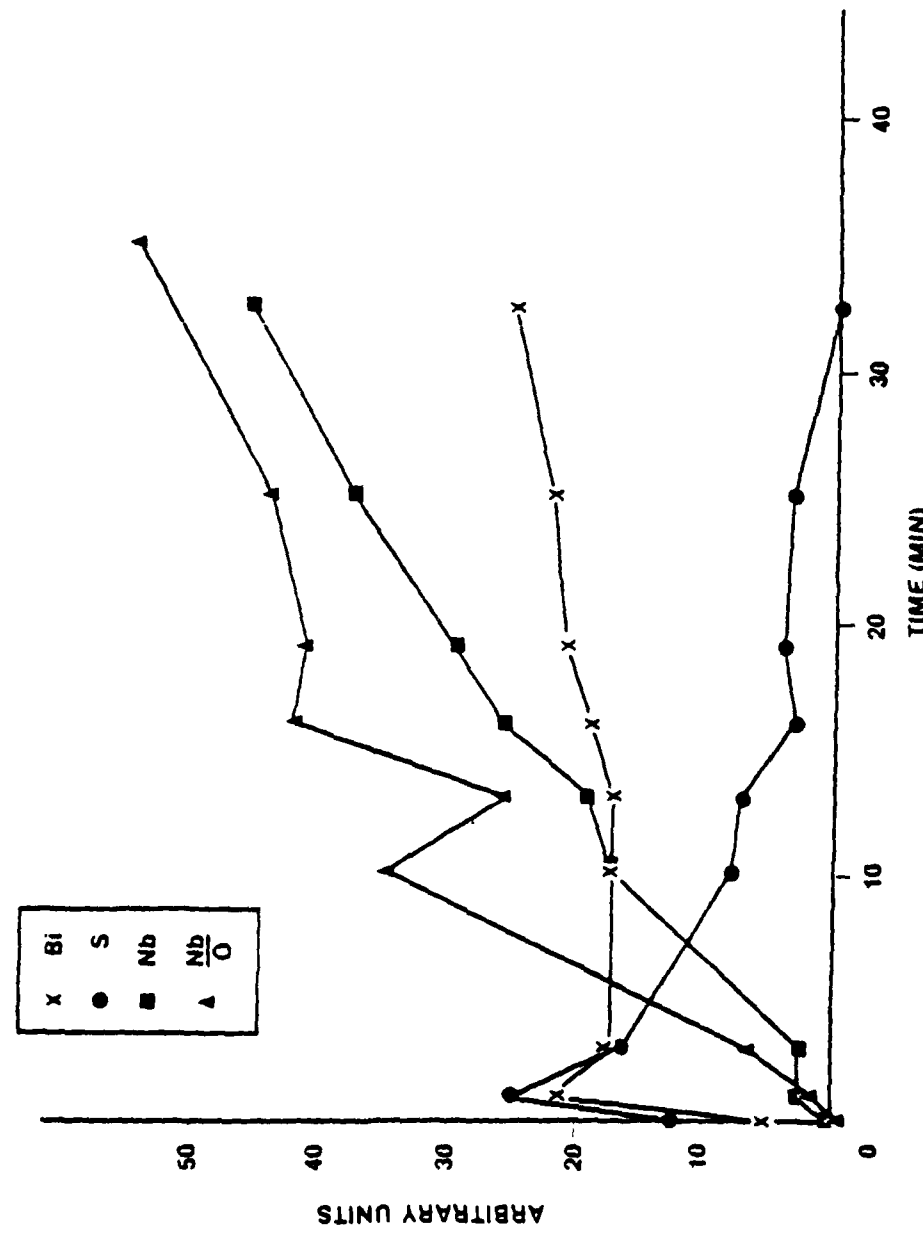


Figure 1.  
AES measurements for a device in the  
structure  $\text{Bi}-\text{NbO}_2-\text{Bi}$ .  
b) After Switching

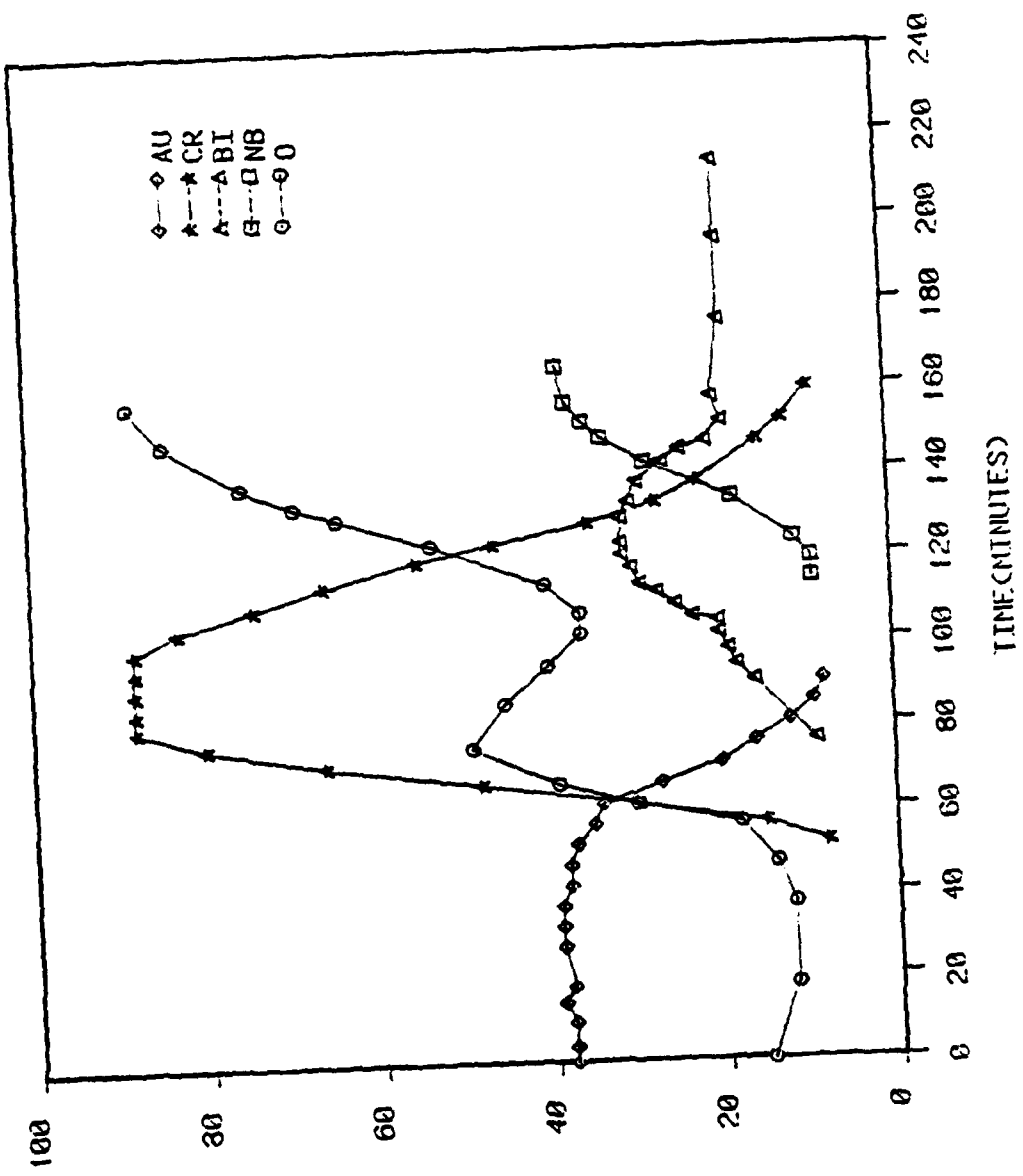


Figure 2. AES analysis of the Au-Cr-Bi-NbO<sub>2</sub>-Au polycrystalline device  
a) before switching

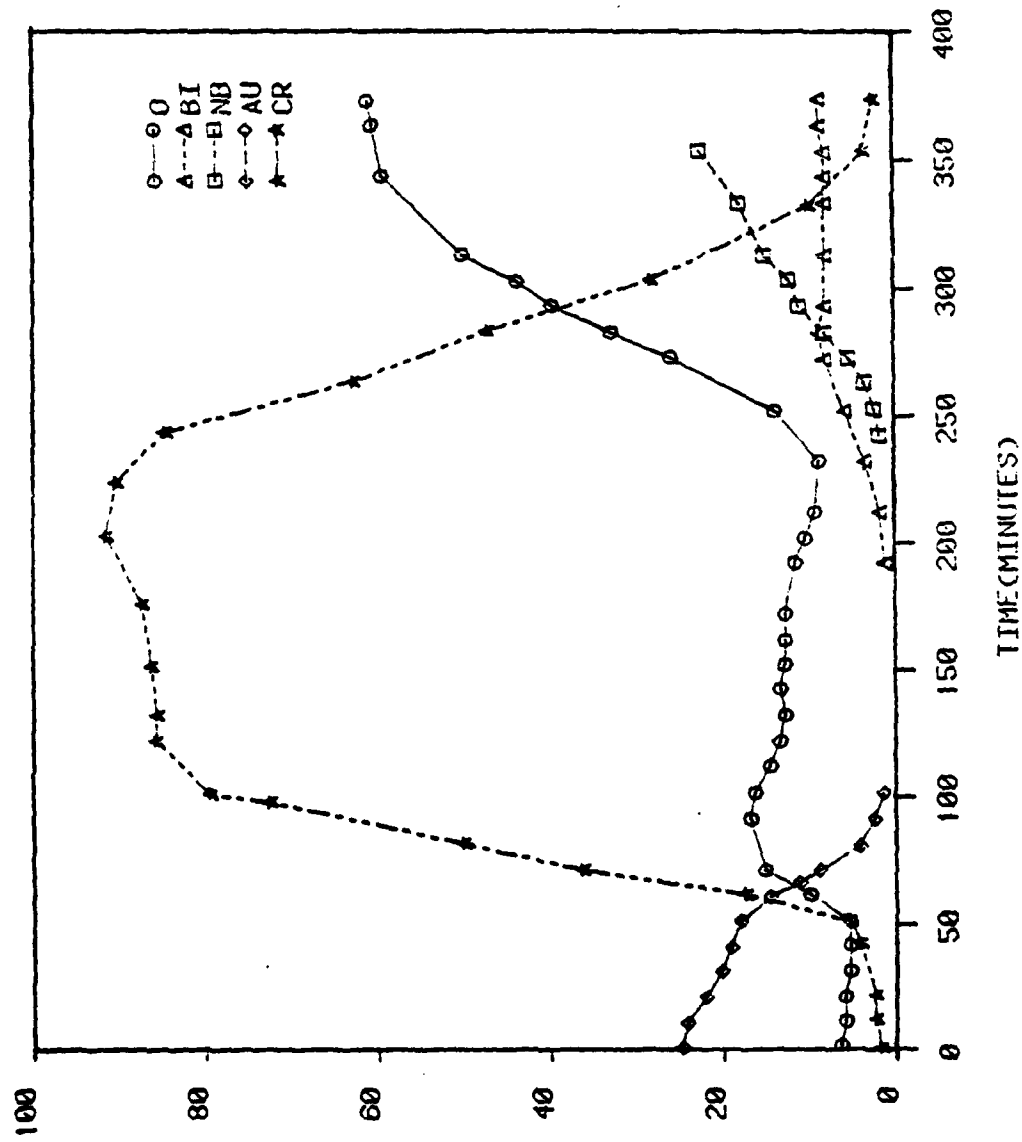


Figure 2. AES analysis of the Au-Cr-Bi-NbO<sub>2</sub>-Au polycrystalline device  
b) after switching

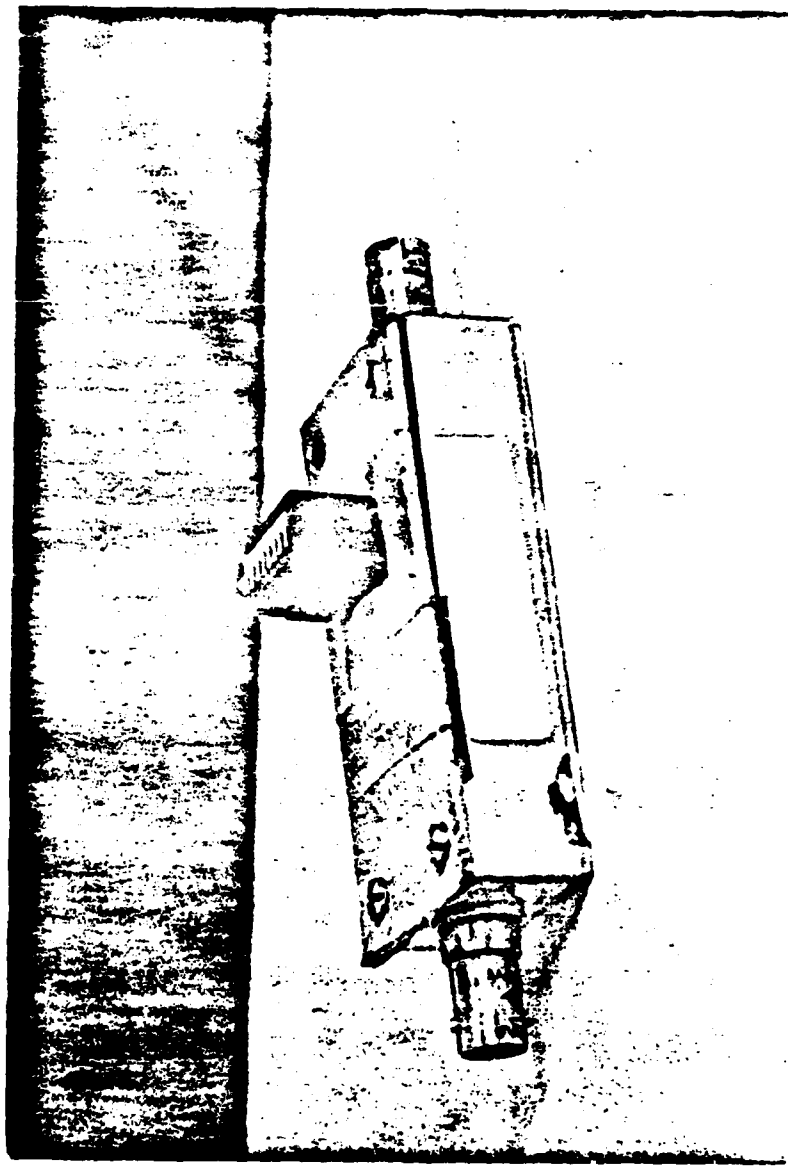
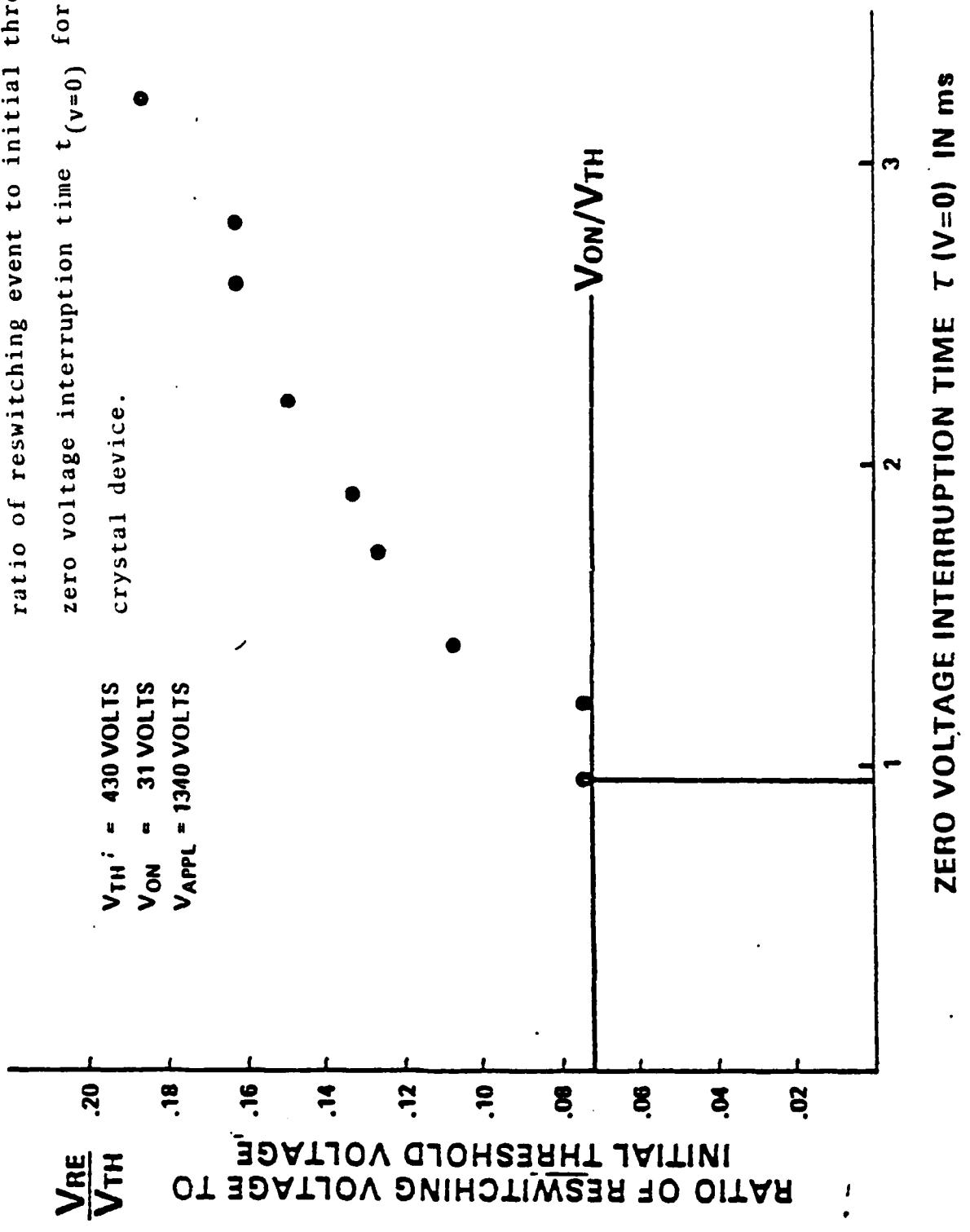


Figure 3. A device packed in MODPACK unit, showing an 8-position microswitch.

Figure 4. Plot of actual recovery curve (or ratio of reswitching event to initial threshold vs zero voltage interruption time  $t$  ( $V=0$ ) for single crystal device.



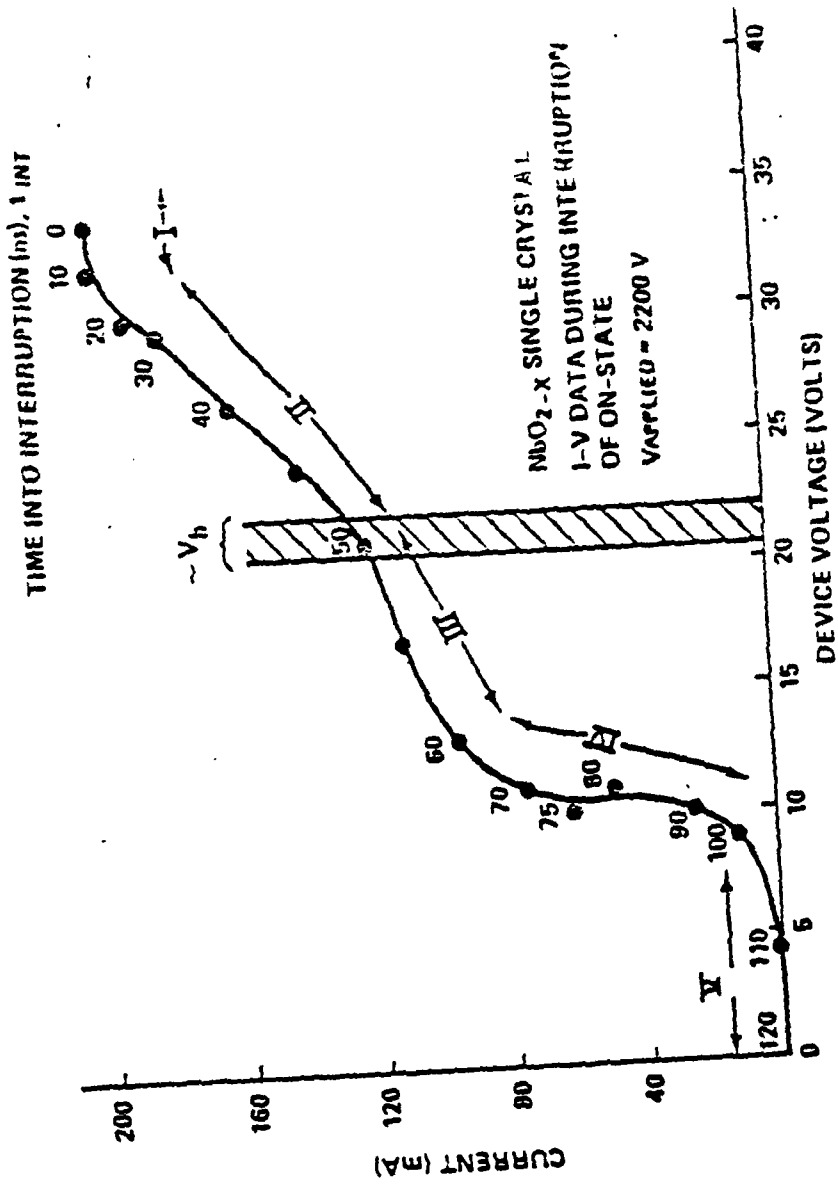


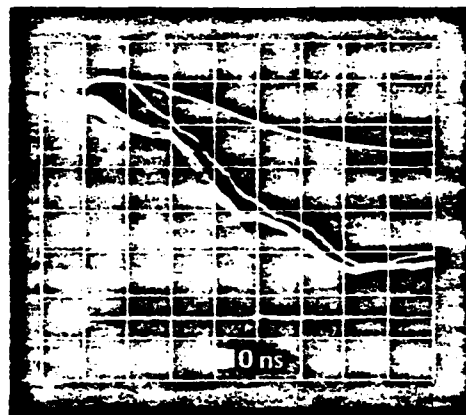
Figure 5. On state I-V-t for Nb<sub>2</sub>O<sub>5</sub> single crystal threshold switch.

CURRENT  
CURRENT GROUND  
DEVICE VOLTAGE  
APPLIED VOLTAGE  
DEVICE VOLTAGE  
GROUND



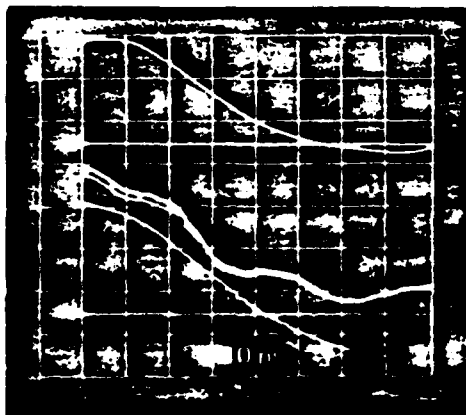
(a)

CURRENT  
DEVICE VOLTAGE  
DEVICE VOLTAGE  
GROUND



(b)

CURRENT  
CURRENT GROUND  
DEVICE VOLTAGE  
APPLIED VOLTAGE  
DEVICE VOLTAGE  
GROUND



(c)

Figure 6. Oscilloscopes for single crystal device showing current (upper trace 40 mA/div), device voltage (middle trace, 5V/div), and applied voltage (lower trace, arbitrary scale) versus time (20ns/div) plus ground lines for current and for device voltage.

TEMP. MEASUREMENT ACROSS ELECTRODES+OBJ. LENS=7.4X RMS. 0.1431  
INFRARED RADIOMETRIC MICROSCOPE-BARNES THIS.

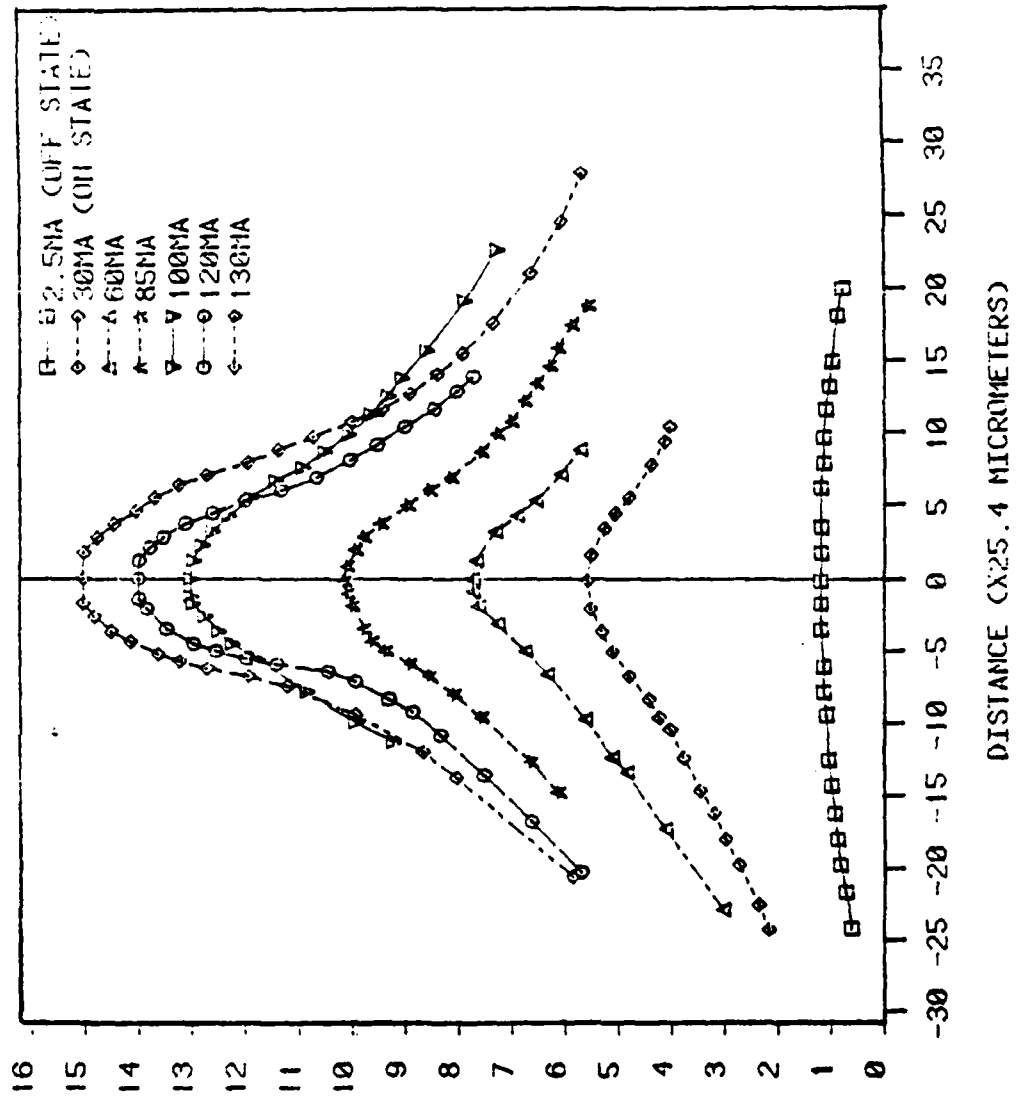


Figure 7.